Sheet Metal Forming—Processes and Applications
T. Altan and A.E. Tekkaya, editors

CHAPTER 7

Hot Stamping

A. Naganathan, Cummins Engine Company
L. Penter, University of Dresden, Germany

IN THE AUTOMOTIVE INDUSTRY, to improve vehicle safety and reduce fuel consumption, manufacturing of lightweight body parts from ultrahigh-strength steels (UHSS) is rapidly increasing. Forming of UHSS at room temperature is limited by low formability and considerable springback. Therefore, hot stamping is accepted as a viable alternative solution and widely used (Fig. 7.1). "Hot stamping is a non-isothermal forming process for sheet metals, where forming and quenching take place in the same forming step" (Ref 7.2). This process takes advantage of low flow stress of boron-alloyed steel (22MnB5) in austenitic phase at elevated temperature and allows the manufacturing of parts with ultrahigh strength, minimum springback, and reduced sheet thickness.

Hot stamping was developed and patented in 1977 by a Swedish company (Plannja), which used the process for saw blades and lawn mower blades (Ref 7.3). In 1984, Saab Automobile AB was the first vehicle manufacturer who adopted a hardened boron steel component for the Saab 9000 (Ref 7.4). The number of produced parts increased from 3 million parts per year in 1987 to 8 million parts per year in 1997, which further increased to approximately 107 million parts per year in 2007 (Ref 7.5).

There are two different methods of hot stamping: direct and indirect.

Direct Method. In the direct method (Fig. 7.2), the blanks are austenitized at temperatures between 900 and 950 °C (1650 and 1740 °F) for 4 to 10 min inside a continuous-feed furnace

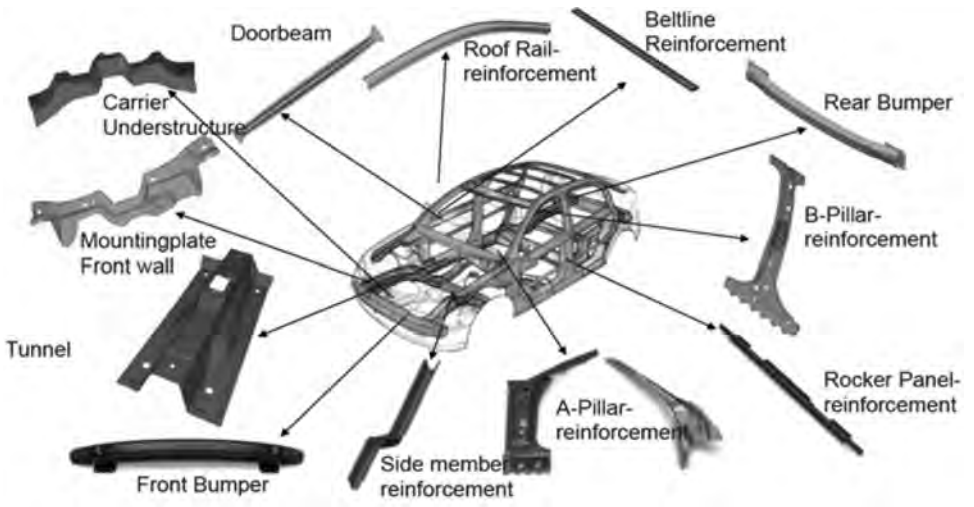

Fig. 7.1 Components manufactured using hot stamping. Source: Ref 7.1

and subsequently transferred to an internally cooled die set via a transfer unit. The transfer usually takes less than 3 s. At high temperature (650 to 850 °C, or 1200 to 1560 °F), the material has high formability, and complex shapes can be formed in a single stroke. The blanks are stamped and cooled down under pressure for a specific amount of time according to the sheet thickness after drawing depth is reached. During this period, the formed part is quenched in the closed die set that is internally cooled by water circulation at a cooling rate of 50 to 100 °C/s (90 to 180 °F/s), completing the quenching (martensitic transformation) process. The total cycle time for transferring, stamping, and cooling in the die is 15 to 25 s. The part leaves the hot stamping line at approximately 150 °C (300 °F) and with high mechanical properties of 1400 to 1600 MPa (200 and 230 ksi) and a yield strength between 1000 and 1200 MPa (145 and 175 ksi).

Indirect Method. Unlike the direct process, indirect hot stamping (Fig. 7.3) provides a part to be drawn, unheated, to approximately 90 to 95% of its final shape in a conventional die, followed by a partial trimming operation, depending on edge tolerance. Then, the preforms are heated in a continuous furnace and quenched in the die. The reason for the additional step is to extend the forming limits for very complex shapes by hot forming and quenching the cold-formed parts.

7.1 Significant Process Variables

Temperature Transformation Curve. The continuous time-temperature transformation curve

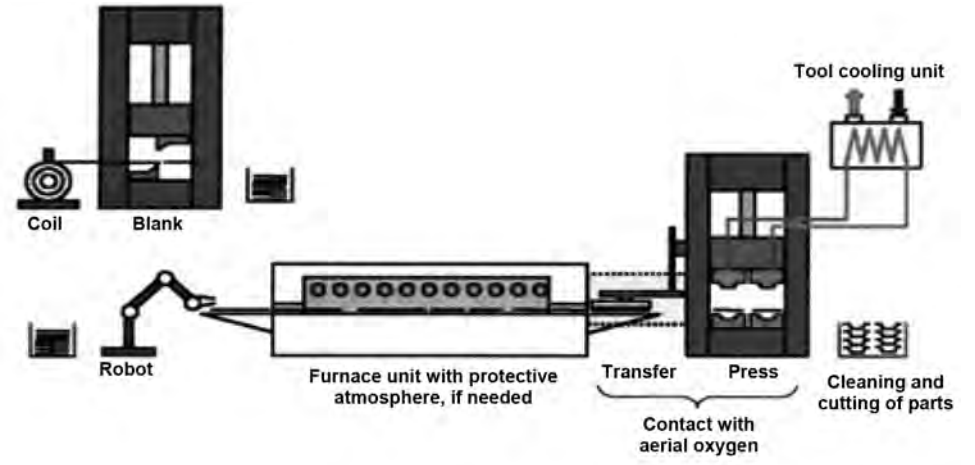

Fig. 7.2 Direct method of hot stamping. Source: Ref 7.6

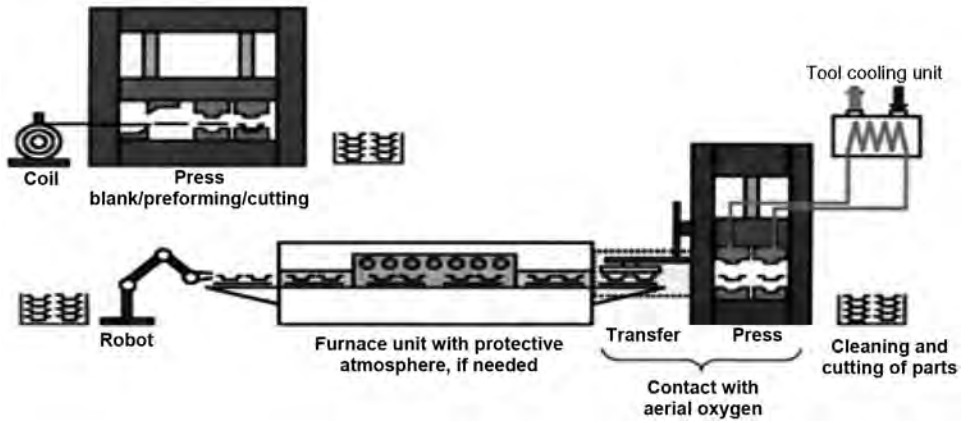

Fig. 7.3 Indirect method of hot stamping. Source: Ref 7.6

illustrates the microstructural evolution of a particular material, depending on the cooling rate. To reach tensile strength up to 1600 MPa (230 ksi) of the final part, a complete transformation of the austenitic to martensitic microstructure is required. Therefore, cooling rates faster than 27 K/s (49 °F/s) in the part must be achieved to avoid bainitic or even ferritic-pearlitic transformation, as shown in Fig. 7.4.

Chemical Composition of 22MnB5. The addition of boron into the steel alloy lowers the critical cooling rate and therefore extends the process window (Table 7.1). Furthermore, alloying boron reduces the carbon equivalent and therefore increases the weldability. Chrome and manganese increase the tensile strength of the quenched material.

Flow-Stress Data for 22MnB5. Reliable finite-element simulation of the hot stamping process requires accurate flow-stress data. For 22MnB5 steel, flow-stress data were obtained as a function of temperature, strain, and strain rate using a modified Gleeble system (Fig. 7.5) (Ref 7.2, 7.8, 7.9).

The rolling direction does not have any influence on the flow-stress data. Temperature has strong influence on the flow stress, as given by the experimental values in Fig. 7.6.

With increase in temperature, there is a decrease in the flow-stress values and the work-hardening exponent. Furthermore, the curve shows an asymptotic trend around 700 to 800 °C (1290 to 1470 °F). This behavior is due to the temperature-induced dynamic, microstruc-

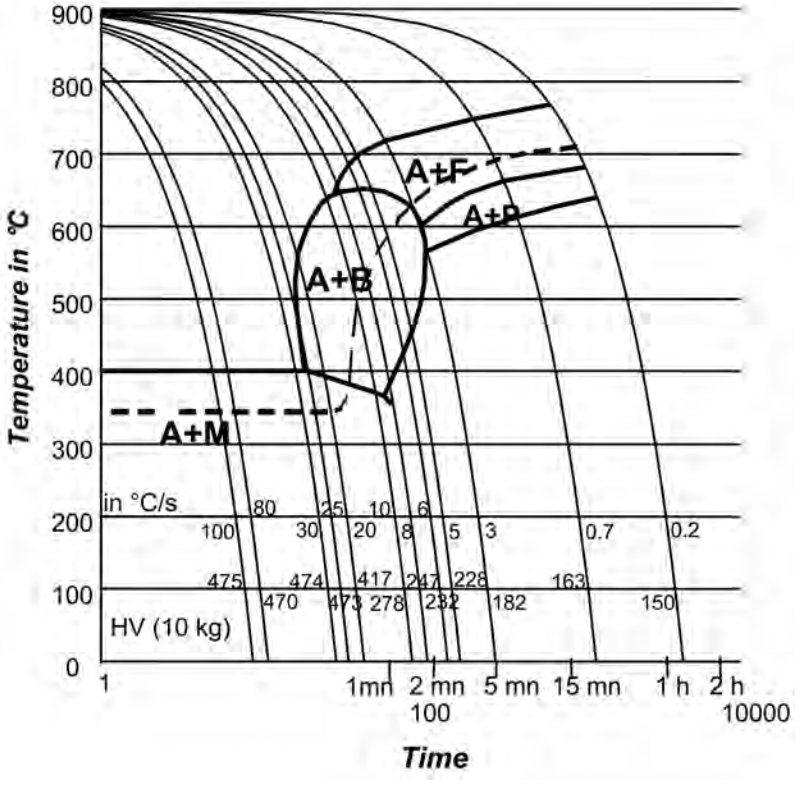

Fig. 7.4 Continuous cooling transformation diagram of 22MnB5 from Arcelor. A, austenite; B, bainite; F, ferrite; P, pearlite; M, martensite. Source: Ref 7.2

Table 7.1 Chemical composition of USIBOR 1500 (1.2 mm, or 0.047 in., thick)

	Composition, wt%											
Material	**C**	**Mn**	**Si**	**Ni**	**Cr**	**Cu**	**S**	**P**	**Al**	**V**	**Ti**	**B**
USIBOR	0.221	1.29	0.28	0.013	0.193	0.01	0.001	0.018	0.032	0.005	0.039	0.0038

Source: Ref 7.7

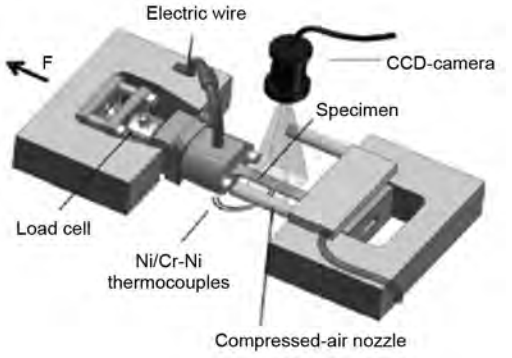

Fig. 7.5 Modified Gleeble 1500 system. CCD, charge-coupled device. Source: Ref 7.2

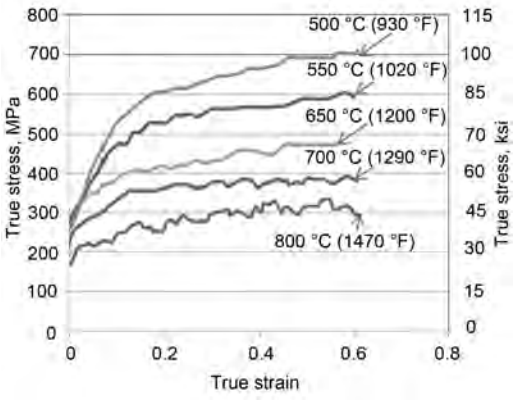

Fig. 7.6 Influence of temperature on flow-stress data. Cooling rate = 80 K/s (145 °F/s); strain rate = 0.1 s^{-1}. Source: Ref 7.9

tural recovery process balancing the strain-hardening effect.

Increase in strain rate increases the flow-stress level and strain-hardening exponent (Fig. 7.7). Increase in the strain-hardening exponent is due to the short annihilation or recovery time available during the test.

At 500 °C (930 °F), the lowest strain rate, 0.01 s^{-1}, leads to higher flow-stress values, as shown in Fig. 7.8.

The reason for significant increase of flow stress at strain rate 0.01 s^{-1} is due to the sudden initiation of the microstructural transformation from austenite to bainite. For higher strain rates, deformation takes place in the austenitic phase, and the flow-stress values show conventional behavior (Ref 7.9).

To study the effect of cooling rate, tests were conducted at an air cooling rate of 15 K/s (25 °F/s) and a rapid cooling rate of 80 K/s (145 °F/s); the results are shown in Fig. 7.9. At 650 and 800 °C (1200 and 1470 °F), the flow-stress values have no effect on the cooling rate. At 500 °C (930 °F), bainite formation caused an increase of flow stress at the lower cooling rate of 15 K/s.

Friction Coefficient. The friction coefficient is an important parameter for calculating accurate material flow and heat transfer during hot stamping simulation. The friction coefficient under relevant conditions of hot stamping is calculated using a tribosimulator (Ref 7.10) and the modified cup drawing test (Ref 7.11). Figure 7.10 represents a schematic of the testing machine used for determining friction in hot stamping (Ref 7.10).

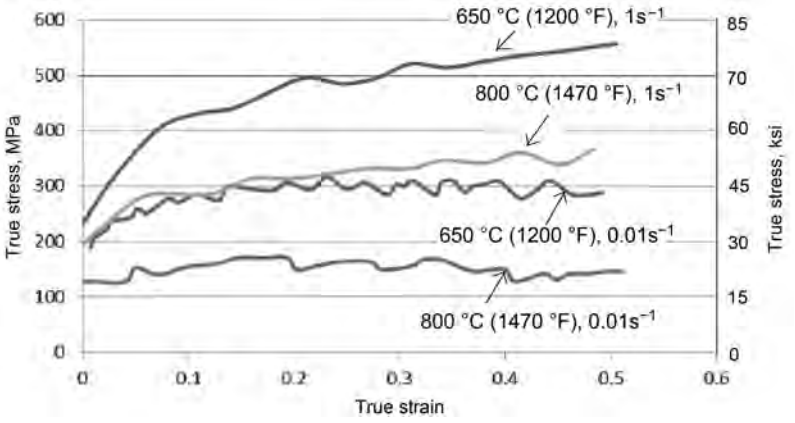

Fig. 7.7 Influence of strain rate. Cooling rate = 80 K/s (145 °F/s). Source: Ref 7.9

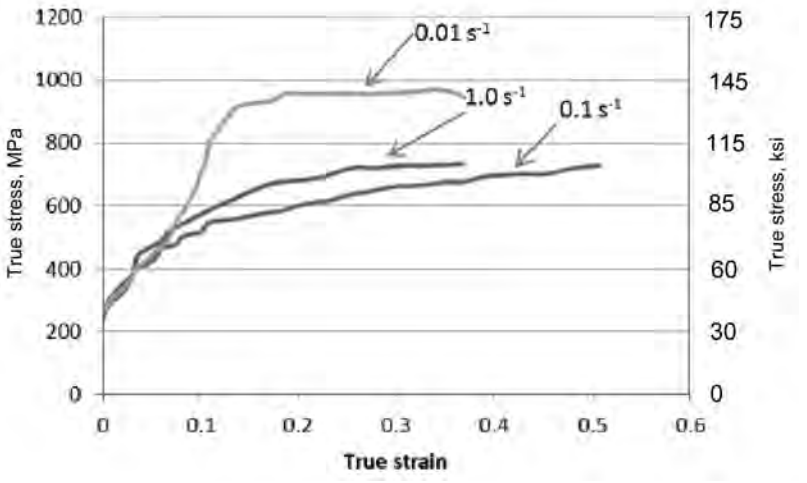

Fig. 7.8 Influence of strain rate at 500 °C (930 °F). Cooling rate = 80 K/s (145 °F/s). Source: Ref 7.9

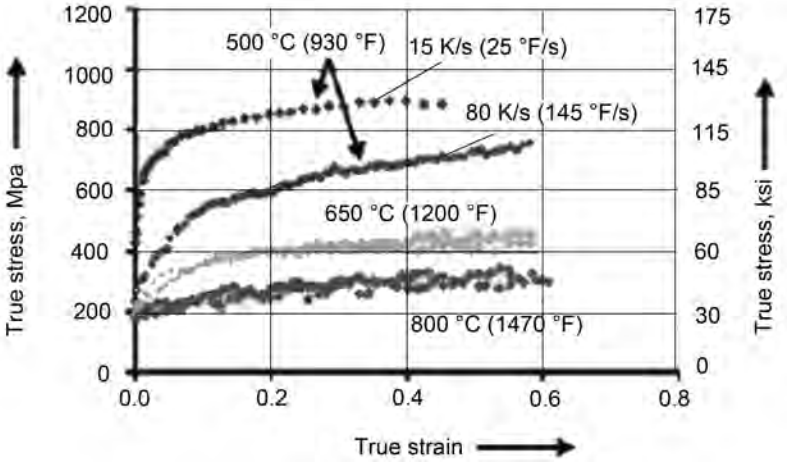

Fig. 7.9 Influence of cooling rate. Source: Ref 7.9

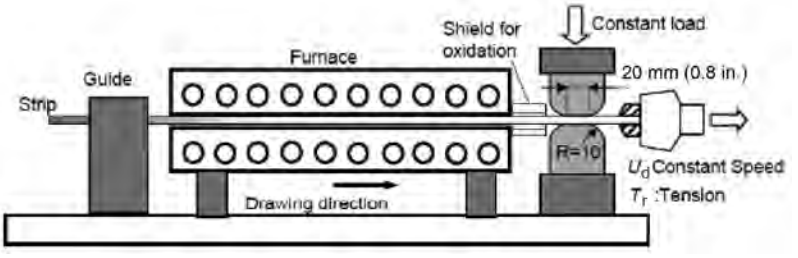

Fig. 7.10 Schematic of testing machine used to determine friction in hot stamping. Source: Ref 7.10

The 22MnB5 sheet material is heated in the infrared furnace to its austenitization temperature under inert gas atmosphere. One end of the strip is clamped with the chuck of the tension device and is pulled at constant speed. Once the heated zone of the strip reaches the entrance of the die, a constant compression load, P, is applied. The coefficient of friction, μ, is calculated from the constant compression load, P, and tension load, T_F, using:

$$\mu = T_F/2P \quad \text{(Eq 7.1)}$$

The experiments were conducted under dry condition without lubricants.

Figure 7.11 shows that with an increase in temperature, there is an increase in the friction coefficient for 22MnB5 steel, and the effect is small for SPHC steel. This effect is due to the scale thickness generated during preheating.

Figure 7.12 represents a schematic of the modified cup drawing test, which is also suggested for determining the coefficient of friction (Ref 7.11). The tool is connected to a hydraulic press equipped with load cells for measuring the punch force, F_p, and the blank holder force, F_{BH}, during the test. The sheet samples are heated in a furnace. The tests were conducted without applying blank holder force in the flange area of the sheet to avoid unnecessary heat transfer. The tests were conducted with a punch velocity (V_{punch}) of 10 mm/s (0.4 in./s). The temperature of the punch (T_{punch}) was kept constant at room temperature (RT). Each parameter combination was tested at least five times (n = 5).The coefficient of friction is calculated using the equation by Siebel (Ref 7.12) that estimates the maximum deep drawing force.

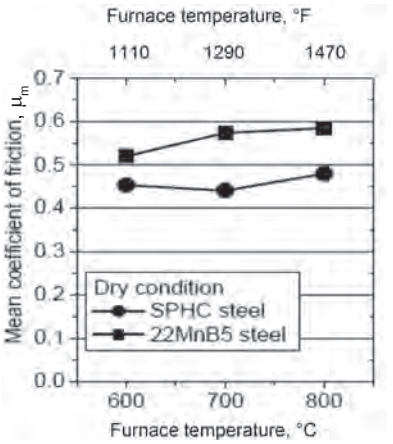

Fig. 7.11 Effect of temperature on mean friction coefficients under dry conditions. Source: Ref 7.10

From Fig. 7.13 and 7.14, it is seen that the friction coefficient decreases with an increase in the temperature of the die and the blank holder. The significant temperature-dependent plastic softening of the material 22MnB5 leads to reduced normal forces transferred from the bulk sheet material to the interacting surfaces at the die. This causes reduction in the friction coefficient with an increase in temperature.

Heat-Transfer Coefficient. The heat transfer between sheet material and die with integrated cooling channels determines the martensite formation and final part properties. The experimental setup for calculating the contact heat-transfer coefficient between sheet materials and die is shown in Fig. 7.15.

The setup contains two water-cooled rectangular plates for quenching the specimen under pressure. The specimen is heated in a furnace to the austenitization temperature of 850 to 950 °C (1560 to 1740 °F) and placed manually on four spring-seated pins. With this experimental setup, the specimens can be loaded during quenching up to a pressure of 40 MPa (6 ksi). The heat-transfer coefficient is calculated using Newton's cooling law, given by:

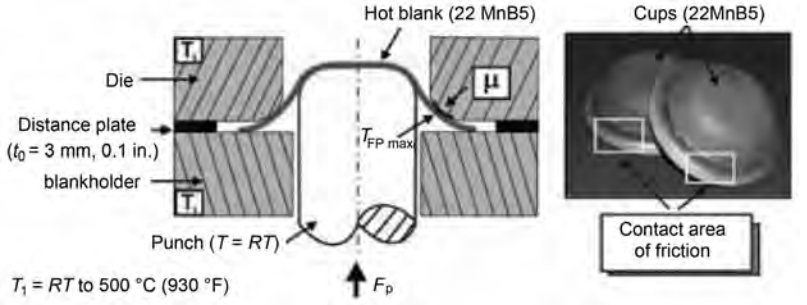

Fig. 7.12 Schematic of experimental setup of the cup deep drawing test (left) and two drawn cups at elevated temperatures (right). Source: Ref 7.11

$$T(t) = (T_0 - T_u) \cdot e^{-\alpha \frac{A}{c_p} t} + T_u \qquad \text{(Eq 7.2)}$$

where T_0 and $T(t)$ are the initial and current temperature of the specimen during the cooling experiment, T_u is the temperature of the contact plates, t is the time during the experiment, A is the geometric contact area, and c_p is the heat capacity of the specimen.

The heat-transfer coefficient, α, is calculated at a particular time, t, from the aforementioned equation, and the corresponding contact pressure is measured from the experiment.

The contact pressure ranges from 0 to 40 MPa (0 to 6 ksi). The specimens were heated to the austenitization temperature of 950 °C (1740 °F) for 5 min. The experiments were repeated for five specimens (n = 5).The heat-transfer coefficient increases as a function of pressure due to the increase in contact surface area; the results are given in Fig. 7.16.

Lechler (Ref 7.14) studied the variation of heat-transfer coefficient as a function of contact distance between die and sheet surface. The results showed that the heat-transfer coefficient between die and sheet material is almost constant (~100 W/m^2 · K) until the contact distance reaches 0.5 mm (0.02 in.), and the value increases steeply to 1200 W/m^2 · K when the die touches the sheet material. The results are given in Fig. 7.17.

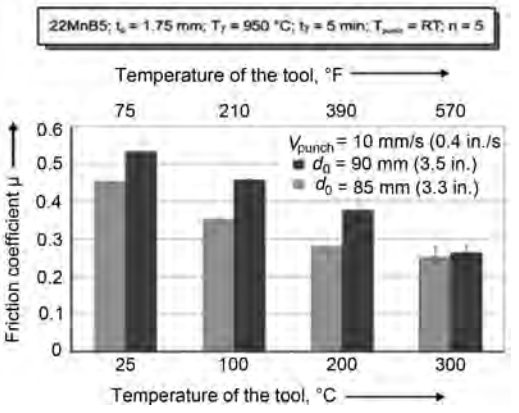

Fig. 7.13 Evolution of friction coefficient, μ, with different tool temperature, maintaining punch at room temperature for 22MnB5. Sheet thickness t_0 = 1.75 mm (0.069 in.); austenitization temperature T_γ = 950 °C (1740 °F); austenitization time t_γ = 5 min; punch velocity V_{punch} = 10 mm/s (0.4 in./s); d_0 = initial blank diameter. Source: Ref 7.11

7.2 Material Flow and Process Simulation

It is important to predict the final properties of the hot-stamped component early in the product development process. If precise predictions of the part geometry and microstructure can be obtained with numerical simulations, it is possible to create components with tailored properties and functionalities in different zones of the

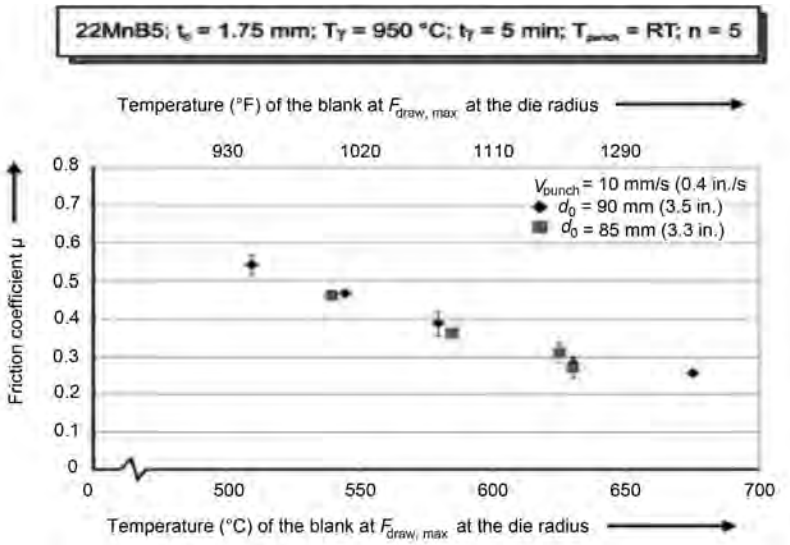

Fig. 7.14 Friction coefficient, μ, as function of blank temperature in contact area at die radius at moment of maximum drawing force for 22MnB5. Sheet thickness t_0 = 1.75 mm (0.069 in.); austenitization temperature T_γ = 950 °C (1740 °F); austenitization time t_γ = 5 min; punch velocity V_{punch} = 10 mm/s (0.4 in./s). Source: Ref 7.11

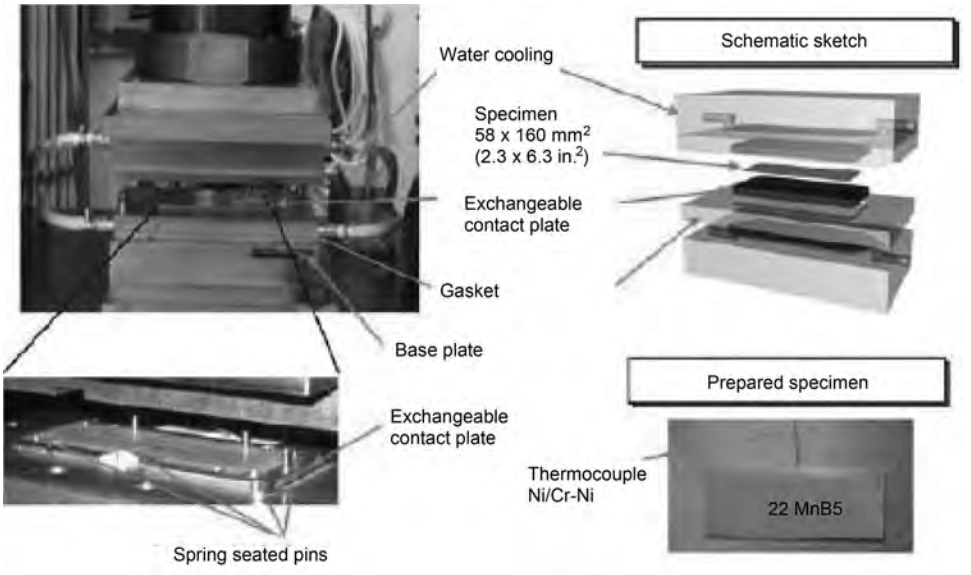

Fig. 7.15 Experimental setup for finding heat-transfer coefficient. Source: Ref 7.13

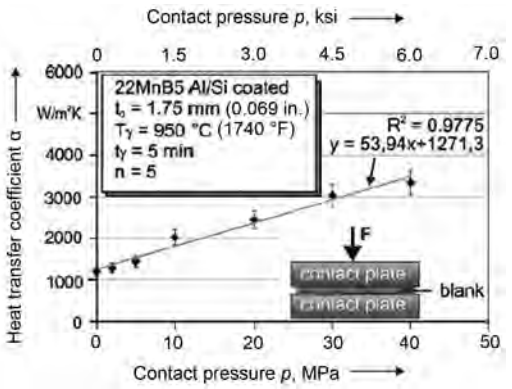

Fig. 7.16 Heat-transfer coefficient as a function of pressure for both-sided metallic contact. Source: Ref 7.11

component. For example, a B-pillar can be manufactured with a softer material zone at its lower end. By allowing controlled buckling in this lower area, severe buckling at a higher location with a possible penetration into the passenger compartment can be prevented (Ref 7.15).

Simulation of Coupled Thermomechanical and Microstructure Evolution. Hot stamping simulation involves combined thermomechanical and microstructure evolution simulation. Hein (Ref 7.16) identified the following challenges in the finite-element simulation of the hot stamping process:

- Temperature - and strain-rate-dependent material parameters (thermal and mechanical)
- Heat transfer between the blank and the die (depending on current contact conditions)
- Coupled thermomechanical calculation
- Evolution of microstructure of the material as a function of temperature, time, and deformation

The interaction between the mechanical field, thermal field, and the microstructure evolution during the hot stamping process is given in the schematic in Fig. 7.18. A description of the different interaction parameters shown in Fig. 7.18 is given in Table 7.2.

The effects of some of the interaction parameters are important, and some parameters can be neglected in the simulation. For example, the heat generation due to plastic deformation and friction can be neglected compared to the overall heat transfer between the blank and the tools (Ref 7.18).

In Table 7.2, parameter 1a, thermal boundary conditions based on deformation, represents the contact heat-transfer coefficient between the die and blank as a function of pressure. Parameter 1b can be neglected in the simulation because of its negligible amount compared to the overall heat transfer between the blank and die. Parameters 2 and 5b can be included in the simulation by considering the variation of thermal dilatation value as a function of temperature. Param-

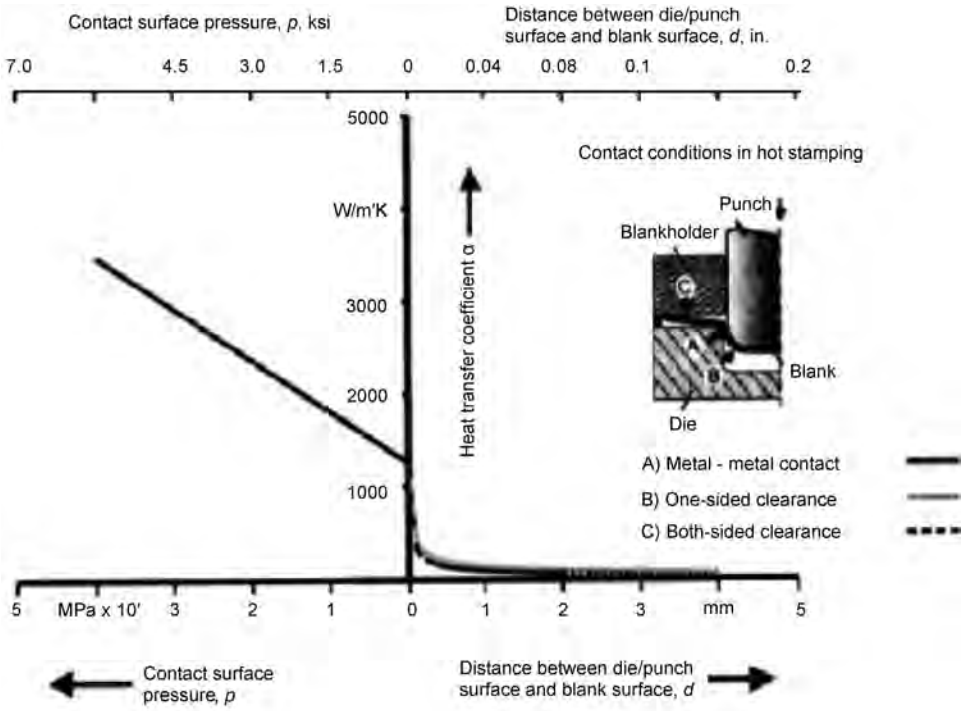

Fig. 7.17 Contact heat-transfer coefficient as a function of contact pressure and distance between tool and sheet material surface. Source: Ref 7.14

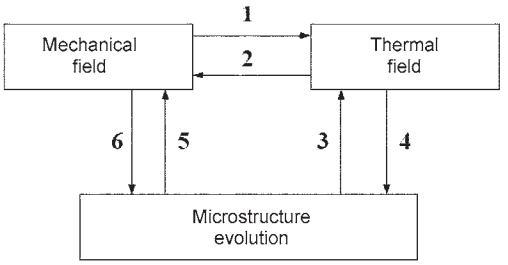

Fig. 7.18 Interactions between the mechanical field, thermal field, and microstructure evolution. Source: Ref 7.17

eter 3a can be included in the simulation by considering the variation of heat capacity of the material with respect to temperature. Parameters 3b and 5a represent the dependency of material parameters on the microstructure evolution based on a certain temperature history. There are two methods of considering these effects in the simulation. First, based on the information of volume fraction of different phases (austenite, ferrite, pearlite, bainite, and martensite) and their properties, the overall material property can be calculated using mixture rules. Secondly, this effect can be considered directly by suitable material characterization experiments following appropriate temperature history. The second method is used widely. Parameter 4 can be calculated from the temperature history and equations such as Koistinen-Marburger (for martensite evolution) (Ref 7.19).

Parameter 5c, transformation plasticity, is an irreversible deformation that occurs when a material undergoes phase transformation under applied stress well below the yield strength of the material. Parameter 5d is not considered in the finite-element simulation.

Table 7.2 Descriptions of interactions in Fig. 7.18

No.	Interaction description
1a	Thermal boundary conditions are deformation dependent.
1b	Heat generation due to plastic dissipation and friction (not accounted for in this work)
2	Thermal expansion
3a	Latent heat due to phase transformations
3b	Thermal material properties depend on microstructure evolution.
4	Microstructure evolution depends on the temperature.
5a	Mechanical properties depend on microstructure evolution.
5b	Volume change due to phase transformations
5c	Transformation plasticity
5d	Memory of plastic strains during phase transformations
6	Phase transformations depend on stress and strain

Source: Ref 7.17

Thermal and Mechanical Properties Required for High-Temperature Forming Simulation (Ref 7.8)

Reliable flow-stress data as a function of strain, temperature, and strain rate for both blank and die material are important for accurate numerical simulation. These data are obtained by tensile test or compression test at high temperature.

Young's Modulus as a Function of Temperature. Young's modulus is a description of the mechanical stiffness of the material. It is temperature dependent and decreases at high temperatures.

Poisson's Ratio as a Function of Temperature. Poisson's ratio relates the axial and lateral strain in uniaxial compression or tension.

Thermal Dilatation due to Thermal Expansion and Phase Transformation. Thermal expansion and volume change due to transformation of austenite to martensite under controlled cooling conditions, evaluated by using dilatation tests, are required for the numerical simulation.

Thermal Conductivity as a Function of Temperature. Thermal conductivity defines the ability of a material to transfer heat. This property is phase and material dependent.

Heat Capacity as a Function of Temperature. The heat capacity of a material represents the amount of energy required to produce a unit temperature rise. This property is phase and temperature dependent. The heat capacity function includes the effects of the latent heat released during transformation from austenite to martensite.

Heat-transfer coefficient between die and sheet material during the hot stamping process changes as a function of distance until the die actually touches the sheet material and as a function of pressure during the deformation process.

Transformation-Induced Plasticity. During phase transformations, the material undergoes plastic deformation even if the applied stress is lower than the yield stress. It occurs by two mechanisms:

- The volume difference between the phases generates internal stresses large enough to cause plastic deformation in the weaker phase (Greenwood-Johnson mechanism).
- The formation of the new phase (martensite in this case) occurs in a preferred orientation that influences the global shape of the material (Magee mechanism).

Constitutive Model for Hot Stamping by Akerstrom

A thermoelastic-plastic constitutive model based on the von Mises yield criterion with associated plastic flow was developed by Akerstrom from Lulea University of Technology, Sweden (Ref 7.20, 7.21). This model includes the effect of austenite decomposition and transformation-induced plasticity. This model is suitable for finite-element simulation using the explicit method.

In this model, the total strain increment during each time step of hot stamping simulation is given by (Ref 7.21):

$$\Delta\varepsilon_{ij} = \Delta\varepsilon_{ij}^{e} + \Delta\varepsilon_{ij}^{th} + \Delta\varepsilon_{ij}^{tr} + \Delta\varepsilon_{ij}^{p} \qquad \text{(Eq 7.3)}$$

where $\Delta\varepsilon_{ij}^{e}$ is the elastic strain increment, $\Delta\varepsilon_{ij}^{th}$ is the thermal strain increment, $\Delta\varepsilon_{ij}^{tr}$ is the isotropic transformation strain increment, and $\Delta\varepsilon_{ij}^{p}$ is the plastic strain increment.

Constitutive Model for Hot Stamping by Behrens

The model developed by Behrens et al. (Ref. 7.22) can be used for implicit simulation methods, which are more efficient for heat-transfer simulations that involve longer duration and small deformations. This model uses the Johnson-Mehl-Avrami equation for diffusion-controlled austenite transformation and the Koistinen-Marburger equation for diffusionless transformation (austenite to martensite). This model was implemented in LS-Dyna version 971. The total strain increment in each step for this thermo-elastic-plastic-metallurgical material model is given by:

$$d\varepsilon_{ij} = d\varepsilon_{ij}^{el} + d\varepsilon_{ij}^{pl} + d\varepsilon_{ij}^{th} + d\varepsilon_{ij}^{tr} + d\varepsilon_{ij}^{tp} \qquad \text{(Eq 7.4)}$$

which is the sum of elastic, plastic, thermal, isotropic transformation, and the transformation-induced plasticity strain increments.

Based on the work from Akerstrom (Ref 7.15, 7.20), material model *MAT_244 was developed and implemented in LS-Dyna for hot stamping application. This model is quite computing-intense. Using this model, final phase and hardness values at different parts of the geometry can be predicted.